Materials Research Bulletin 59 (2014) 267–271

Contents lists available at ScienceDirect

Materials Research Bulletin

journal homepage: www.elsevier.com/locate/matresbu

Enhanced piezoelectric output voltage and Ohmic behavior in Cr-doped ZnO nanorods

Nidhi Sinha [a,b], Geeta Ray [a], Sanjay Godara [a], Manoj K. Gupta [a], Binay Kumar [a,*]

[a] Crystal Lab, Department of Physics & Astrophysics, University of Delhi, Delhi 110007, India
[b] Department of Electronics, SGTB Khalsa College, University of Delhi, Delhi 110007, India

ARTICLE INFO

Article history:
Received 5 March 2014
Received in revised form 15 July 2014
Accepted 18 July 2014
Available online 21 July 2014

Keywords:
A. Nanostructures
C. Atomic force microscopy
C. Transmission electron microscopy (TEM)
D. Ferroelectricity
D. Electrical properties

ABSTRACT

Highly crystalline Cr-doped ZnO nanorods (NRs) were synthesized by solution technique. The size distribution was analyzed by high resolution tunneling electron microscope (HRTEM) and particle size analyzer. In atomic force microscope (AFM) studies, peak to peak 8 mV output voltage was obtained on the application of constant normal force of 25 nN. It showed high dielectric constant (980) with phase transition at 69 °C. Polarization vs. electric field (P–E) loops with remnant polarization (6.18 $\mu C/cm^2$) and coercive field (0.96 kV/cm) were obtained. In *I–V* studies, Cr-doping was found to reduce the rectifying behavior in the Ag/ZnO Schottky contact which is useful for field effect transistor (FET) and solar cell applications. With these excellent properties, Cr-doped ZnO NRs can be used in nanopiezoelectronics, charge storage and ferroelectric applications.

1. Introduction

Zinc oxide (ZnO) has a growing technological importance due to its piezoelectric, semiconducting, optical and dielectric properties. Its properties can be coupled to get various optoelectronic applications including blue/ultra violet (UV) light emitting diodes, UV photo-detectors, high electron mobility transistors, spintronics and energy (nano-) generators [1–7]. ZnO nanostructures are known to exhibit strong piezoelectric and pyroelectric properties for nanogenerator and nanoscale biosensor applications [8–11]. Wang and Song have reported the energy generation from ZnO nanowires by utilizing its semiconducting and piezoelectric properties [10]. Huang et al. have reported applications of ZnO in organic hybrid solar cells [2]. For the performance of various ZnO based electronic devices, ZnO-metal contacts play a crucial role. Usually ZnO-metal contacts show Schottkey barrier with non-linear *I–V* characteristics. Ohmic contact is a challenging requirement for ZnO-based nanostructures. Ohmic contacts are very useful for electronic and photonic devices, such as field effect transistors (FETs), light emitting diodes (LEDs), solar cells, and sensors [12]. A good Ohmic contact has negligible contact resistance relative to the bulk resistance of the semiconductor, and does not significantly reduce the device performances due to a small voltage drop across the contact. This property of Ohmic contact can be achieved in ZnO by inductively coupled hydrogen and argon plasma treatment [13], focused ion beam treatment [14], annealing or by increasing the effective carrier concentration on the surface during growth process [15]. Increased carrier concentration creates oxygen vacancy on the surface of ZnO. In addition, ZnO has several advantages like easy growth, non-toxicity, coupled optoelectronic properties, etc. However, the low polarization in pure ZnO is a cause of concern and, therefore, the interest of research have been focused on achieving large polarization in ZnO by introducing various dopants like K, Mg, Li, Cr and V in the ZnO lattice [16–21]. ZnO is known to have various possible native point defects present in the lattice as interstitial Zn or O (Zn_i or O_i), zinc vacancy (V_{Zn}), oxygen antisite (O_{Zn}), zinc antisite (Zn_O) and oxygen vacancy (V_O) [3,7,15]. The enthalphy of oxygen vacancies formation is low so they are more often present in the system. On the other hand, Zn antisites, O antisites, and O interstitials have high energies of formation so they are not present in large concentration under normal conditions. The defects Zn_i and Zn_O act as shallow donor while oxygen vacancies act as deep donors and zinc vacancies are deep acceptors. Zinc antisites also have a large off-site displacement thus they induce a large local lattice relaxation. The defects acting as donors may spontaneously compensate the deliberately introduced acceptors such as Cr^{3+}. These defects directly or indirectly play an important role in controlling the growth process, doping compensation, minority carrier, luminescence efficiency, electrical properties and can originate ferromagnetism in ZnO. Cr is an important transition

---

[*] Corresponding author. Tel.: +91 9818168001; fax: +91 11 27667061.
E-mail addresses: bkumar@physics.du.ac.in, b3kumar69@yahoo.co.in (B. Kumar).

http://dx.doi.org/10.1016/j.materresbull.2014.07.032
0025-5408/© 2014 Elsevier Ltd. All rights reserved.

metal element and it has close ionic radius parameter to that of Zn^{2+}, which ensures that Cr^{3+} can easily penetrate into ZnO crystal lattice or substitute Zn^{2+} position in the crystal. Here, we report the effect of Cr-doping on the electromechanical performance of ZnO which includes observations of output voltage in EFM studies, dielectric constant, piezoelectric property, ferroelectric property and *I*–*V* characteristic of Cr-doped ZnO.

2. Experimental

Wet chemical solution method was used to synthesize 0.1 M Cr-doped ZnO nanorods (Cr-ZnO NRs) as reported earlier [22]. The structure and crystalline quality were characterized by X-ray diffraction (XRD) with a Bruker D8 Advance Cu $K\alpha_1$, $\lambda = 1.5405$ Å at room temperature. The formation of NRs was confirmed by high resolution transmission electron microscopy (HRTEM) which was carried out by a Tecnai 300 kV Ultra twin 25 (FEI Company) with an attached energy-dispersive X-ray spectrometer (EDX). TEM samples were prepared by dispersing the powder in ethanol by ultrasonic treatment, positioning a drop onto a porous carbon film supported on a copper grid, and then drying it in air. The particle size distribution was analyzed using a Malvern Zetasizer Nano Instruments by making a colloidal solution of ZnO nano-powder in distilled water. The topographical and piezoresponse of the Cr-ZnO NRs was measured using an atomic force microscope (AFM) (Veeco DICP2 instrument) with a Pt coated Si-tip and electric force microscopy (EFM). For dielectric and piezoelectric measurements a pellet of 13 mm diameter and 1 mm thickness was prepared using KBr hydraulic press. Both the surfaces of the pellet were coated with high grade silver paste to provide good electrical contact. Pellet was dried at 373 K for 1 h. Piezoelectric charge coefficient d_{33} was measured by PiezoMeter System (Piezotest PM 300). The dielectric constant of Cr-ZnO NRs was measured using an Agilent E 4980 A LCR meter and Agilent 16060 A test fixture for a frequency range 1 kHz–2 MHz in the temperature range of RT-160 °C. P–E loops were traced by an indigenously-built Sawyer–Tower circuit interfaced with computer controlled loop tracer at room temperature. *I*–*V* characteristic for pure and Cr-ZnO NRs was obtained by applying a dc bias voltage of −20 to 20 V using a Keithley Source Meter (series 2400) across a pellet of ZnO on which Ag-layer has been created.

3. Result and discussion

3.1. Crystal structure

The XRD pattern of the as grown Cr-ZnO NRs at room temperature is shown in Fig. 1. It confirmed the formation of hexagonal system of Cr-ZnO NRs (space group $P6_3mc$). All the diffraction peaks coincide with (JCPDS Card No. 36-1451). The lattice parameters of Cr-ZnO NRs were found to be, $a = 3.249$ Å and $c = 5.206$ Å. The grain size and preferential growth direction etc. have been reported earlier for Cr-ZnO NRs [22].

3.2. Morphology and particle size

Morphology and particle size distribution of the Cr-ZnO NRs were analyzed by high resolution transmission electron microscopy (HRTEM). HRTEM confirmed the well separated distribution of Cr-ZnO NRs as shown in Fig. 2a–c. The average diameter and length of the pure ZnO NRs were found to be around 50 nm and 300 nm, respectively which remain nearly unchanged after the doping of Cr (Fig. 2a and b). However, while the pure ZnO NRs have more uniform dimensions, the Cr-ZnO NRs exhibit visible variations in dimensions and show roughness at their edges. Further, there is no indication of secondary phases and clustering in the HRTEM images, suggesting that all Cr atoms are homogeneously incorporated into the ZnO NRs as evident in a single isolated Cr-ZnO rod (Fig. 2c). The bright diffraction pattern spots were observed in selected area electron diffraction (SAED) pattern of Cr-ZnO NRs as shown in the inset of Fig. 2c, which confirms its single crystalline nature. The EDX spectra of the Cr-ZnO NRs (showing Zn, O, and Cr peaks) confirmed the 0.4 atomic percentage incorporation of Cr into ZnO lattice as shown in Fig. 2d [22].

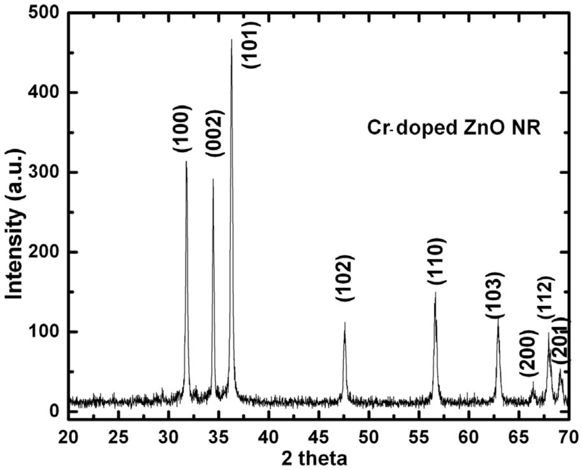

Fig. 1. XRD patterns of Cr-doped ZnO nanorods showing high crystalline nature with no impurity peaks.

The size distribution of the Cr-ZnO NRs was also analyzed from a statistical method based on the quasi-elastic scattering of the light by the particles in a colloidal solution of Cr-ZnO NRs in distilled water using a Malvern Zetasizer Nano Instruments. It was observed that about 70% of the particle has average dimensions of around 300 nm (inset of Fig. 2d). The size of the nanoparticles is comparable with the size obtained in the HRTEM (Fig. 2a and b). Since the shape of Cr-ZnO NRs is of a cylindrical form while the statistical method takes into account of a spherical shape, thus the size distribution obtained from the Malvern Zetasizer is a reflection of an average of the diameter and length of Cr-ZnO NRs.

3.3. Atomic force microscopy and piezoelectricity

The topographical and piezoresponse of the Cr-ZnO NRs was measured using an atomic force microscope (AFM) (Veeco DICP2 instrument) with a Pt coated Si-tip. In the AFM contact mode, a constant normal force of 25 nN was applied between the tip and the sample surface. The spring constant of the cantilever was calibrated to be 2.0 N/m. Fig. 3a and b displays the atomic force microscopy (AFM) and electric force microscopy (EFM) images of a Cr-ZnO NRs. Inset of Fig. 3a shows the schematic diagram of the voltage generation as a result of the bending of the NRs. We employed the electric force microscopy (EFM) to measure the induced surface charges of Cr-ZnO NRs, which is related to the piezoelectric and ferroelectric properties of the sample. Furthermore, EFM technique is used to detect the local variation in surface charges which is induced by the strain due to piezoelectricity. The roughness (root mean square deviation of the surface Sq) of the topographical image taken by AFM mode was found to be 56.45 nm by using SPIP V5.1.2.0 software (Fig. 3a). The output image of AFM shown in Fig. 3b was recorded simultaneously when the AFM tip was scanned over the Cr-ZnO NRs over a scanned area $20 \times 20\ \mu m^2$. In Fig. 3b, the topography (blue curve) and corresponding output voltage (black curve) line profiles of Cr-ZnO NRs are shown. Each peak represents an electric